Earth and Planetary Science Letters, 98 (1990) 319–328
Elsevier Science Publishers B.V., Amsterdam – Printed in The Netherlands

[XLeP]

Magnetic transition at 30–34 Kelvin in pyrrhotite: insight into a widespread occurrence of this mineral in rocks

Pierre Rochette [a], Gérard Fillion [b], Jean-Luc Mattéi [b] and Marinus J. Dekkers [c]

[a] *LGIT, Observatoire de Grenoble, IRIGM BP 53X 38041 Grenoble Cedex (France)*
[b] *Laboratoire de Magnétisme Louis Néel, CNRS, 166X 38042 Grenoble Cedex (France)*
[c] *Paleomagnetic Laboratory "Fort Hoofddijk," University of Utrecht (The Netherlands)*

Received October 23, 1989; revised version accepted February 15, 1990

A characteristic magnetic transition at 30–34 K is shown to provide a powerful tool for the identification of pyrrhotite with concentration down to 10 ppm through the same low-temperature techniques as applied to magnetite and hematite, extended down to liquid helium temperature. A review of rock magnetic and petrological data on pyrrhotite suggests that this mineral should be considered as a major carrier of paleomagnetic signals. Unblocking temperature up to 350 °C and extreme resistance against AF may be encountered in fine grained pyrrhotite.

1. Introduction

Although the magnetic and physical properties of ferrimagnetic iron sulfides and especially monoclinic pyrrhotite (Fe_7S_8) have been rather extensively described [1–6], pyrrhotite is quoted as a minor magnetic mineral in most paleomagnetic textbooks. In fact, as will be discussed in this paper, the prevalence of pyrrhotite, its strong and stable magnetic properties make it potentially as important as magnetite as carrier of a paleomagnetic signal.

Although pyrrhotite has a saturation magnetization ($M_s = 15$ A m^2/kg) six times smaller than that of magnetite, its remanence is comparable. This is because the M_{rs}/M_s ratio varies from 0.2 to 0.6 depending on grain size while this ratio in magnetite has much lower values. Also the specific thermo-remanence (TRM) in the earth's magnetic field amounts to 10^{-2} to 0.3 A m^2/kg [6], and can equal the values of 10^{-2} to 1 A m^2/kg for magnetite [7]. Amounts of pyrrhotite of the order of 10^{-4} or less are thus sufficient to account for the natural remanence (NRM) of weakly magnetic rocks. Therefore every rock where sulfides are thermodynamically stable is prone to show a significant paleomagnetic signal due to pyrrhotite even if this mineral is not detected by the usual mineralogical techniques.

2. Occurrence of pyrrhotite in rocks

Pyrrhotite is an important redox and temperature indicator [8,9] in diagenetic, metamorphic and magmatic conditions. It is rather ubiquitous in economic sulfidic ores but also occurs as an accessory mineral in many rock types.

The stable iron sulfide in magmatic rocks is hexagonal antiferromagnetic pyrrhotite (Fe_9S_{10}), which easily turns into Fe_7S_8 and eventually smythite (Fe_9S_{11}, also ferrimagnetic [1]) during low temperature alteration [9,10]. Pyrrhotite has been reported in granites [10], in basaltic dikes [11], and in peridotites [12]. It is also quite common in deep crustal rocks including serpentinites and granulites [13].

Primary magnetization carried by pyrrhotite has been reported in sediments [14] although sedimentologists usually found that the stable authigenic sulfides are restricted to pyrite (FeS_2), mackinawite (FeS_{1-x}) and greigite (Fe_3S_4) [15] among which only greigite is ferrimagnetic [1]. Indeed pyrrhotite is more typical of later evolution, such as the decay of the less stable authigenic sulfide into pyrite and pyrrhotite. Two metamorphic reactions producing pyrrhotite have been recognized in black shales and dark limestones [9]: (1) the transformation of primary magnetite in the presence of pyrite and organic matter, observed in the

lower greenschist facies (about 300°C), and (2) the breakdown of pyrite (about 400°C). Minor amounts of pyrrhotite may appear from pyrite at much lower temperatures [16]. Pyrrhotite derived from gypsum has also been reported in anchizonal metasediments [17]. All those reactions may lead to very stable secondary magnetizations in slightly metamorphosed sedimentary rocks situated in orogenic belts where reliability of paleomagnetic data is of key geodynamic importance [e.g. 18–20].

3. Rockmagnetic properties and identification criteria for pyrrhotite

Fe_7S_8 is ferrimagnetic, due to vacancy ordering, with a maximum Curie temperature (T_c) at 325°C as shown by the thermomagnetic curves in Fig. 1

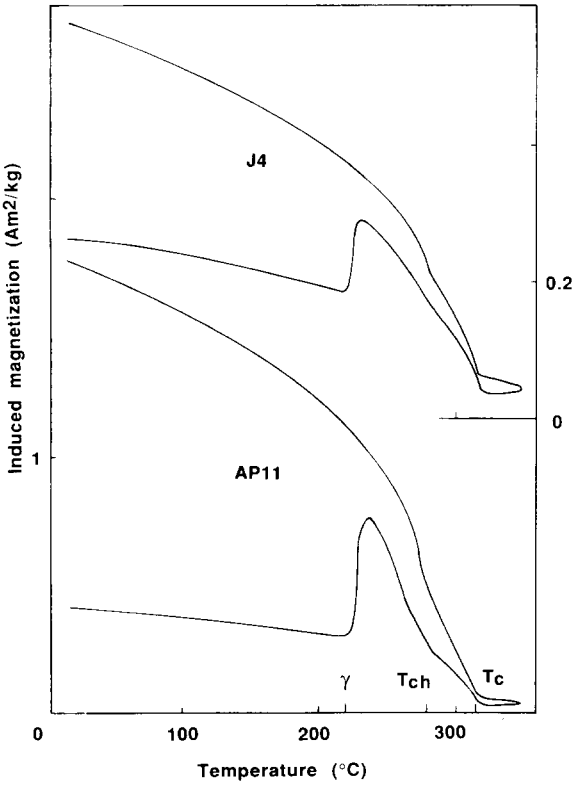

Fig. 1. Thermomagnetic curves of rock samples J4 and AP11 showing the Curie temperatures of hexagonal (T_{ch}) and monoclinic (T_c) pyrrhotites together with the g transition on hexagonal pyrrhotite. Inducing field: 0.8 T, heating and cooling in vacuum at a rate of 1°/min, except cooling below 250°C where a rate of 5°/min were used to quench the hexagonal pyrrhotite into its ferrimagnetic metastable form.

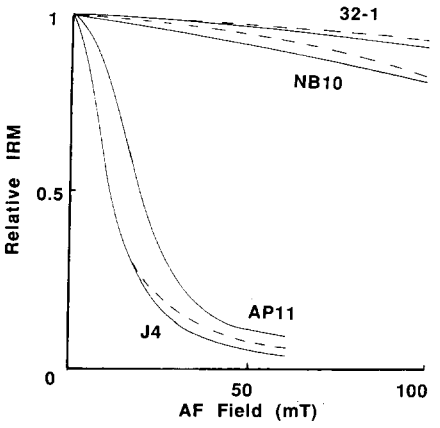

Fig. 2. AF demagnetization curves of saturation IRM before (solid line) and after liquid helium temperature cycling (dashed line) in four pyrrhotite bearing rock samples (including those of Fig. 1; see Table 1).

(see Table 1 for sample description). Curie points down to 310°C are observed, depending on substitution and slight variations in the Fe/S ratio [2]. The critical size for single domain is estimated at 3 μm [11]. Pyrrhotite shows a wide range of remanent coercive force (H_{cr}) according to grain size [4,5]. The behavior under alternating fields (AF) of rock samples that yield H_{cr} from 6 to 250 mT is presented in Fig. 2. Saturation of isothermal remanence (IRM) is reached below 1.2 T even for the hardest samples.

Pyrrhotite, even in large multi-domain grains, is characterized, as hematite, by its ability to acquire a large remanence. When hysteresis curves are able to provide values of M_s, coercive force (H_c) and initial susceptibility (K_0), the following criteria are useful to discriminate between pyrrhotite and magnetite: (1) for all the grain size range of pyrrhotite $M_{rs}/M_s > 0.2$, $H_{cr}/H_c < 1.5$ and $M_{rs}/K_0 > H_{cr}$; and (2) for magnetite $M_{rs}/M_s < 0.2$, $H_{cr}/H_c > 2$ and $M_{rs}/K_0 < H_{cr}$ unless the grains are single-domain and strongly anisotropic.

Soft multi-domain pyrrhotite in schists [9] exhibits anhysteretic susceptibility (K_a) as high as 24 times K_0. Unpublished measurements in the set of sized dispersed samples TTE [5] yield values of K_a/K_0 increasing from 4 to 10 with decreasing grain size from 150–250 μm to less than 5 μm. These values are quite different from magnetite values which hardly exceed 10 and are less 1 for multi-domain grains [21]. With the onset of nor-

TABLE 1
Characteristics of the studied pyrrhotite samples

Sample	Origin and reference	T_c (°C)	T_π (K)
Monocrystal 30	Sphere of $f = 3$ mm (Pauthenet) [25]	315	30
OR1(p)	Synthetic (Orléans)	320	32
EOR(p)	Ore, Elba (Italy) [5]	325	34
TTE(p)	Ore, Temporino (Italy) [5]	325	34
Rouez(p)	Ore, Brittany (France)	320	34
J4(r)	Black schist, Jurassic (Switzerland) [9]	320	30
AP11(r)	Black schist, Precambrian (Tennessee) [31]	320	33
72A(r)	Granite (Algeria) [a] [24]	325	32
NB10(r)	Limestone, Jurassic (French Alps) [19]	≤ 350	34
32.1(r)	Limestone, Carboniferous (Nepal) [b]	≤ 350	32
OW2.A	Limestone, Silurian (Appalaches) [33]	≤ 350	34

(p) = sized dispersed powder; (r) = rock sample; maximum unblocking temperature is indicated for the last three samples.
[a] A. Arafa, pers. commun.
[b] E. Appel, pers. commun.

malization methods to identify the origin of NRM [22] it is worth pointing out that a pyrrhotite TRM acquired in the earth field is quite high relative to IRM: TRM/IRM ratios from 1 to 6% depending upon grain size, are observed in sized dispersed fractions [6].

Other criteria to identify pyrrhotite are its non-vanishing rotational hysteresis [16,23] and the quite common coexistence of the hexagonal and monoclinic form. The hexagonal form is unambiguously detected by its thermomagnetic behavior (Fig. 1 and [2]) due to the so called γ transition at $T_\gamma = 200–220$ °C from the low-temperature antiferromagnetic form to a ferrimagnetic form with a Curie point T_{ch} at 275–295 °C, significantly lower than T_c of the monoclinic form. The γ transition is also easily detected by a susceptibility increase after quenching from a temperature higher than T_γ [9].

However, the only pertinent measurable magnetization in weakly magnetic rocks is the remanence, because paramagnetic contributions strongly contaminate susceptibility and induced magnetization [24]. The use of only blocking temperature (T_b) and coercivity spectra of NRM or IRM may lead to a confusion with titanomagnetite. Moreover the estimation of the maximum T_b characterizing pyrrhotite is hampered by the common coexistence of pyrrhotite with magnetite, by the onset of unstable magnetization around 350°C due to oxidation of sulfide to magnetite, and by

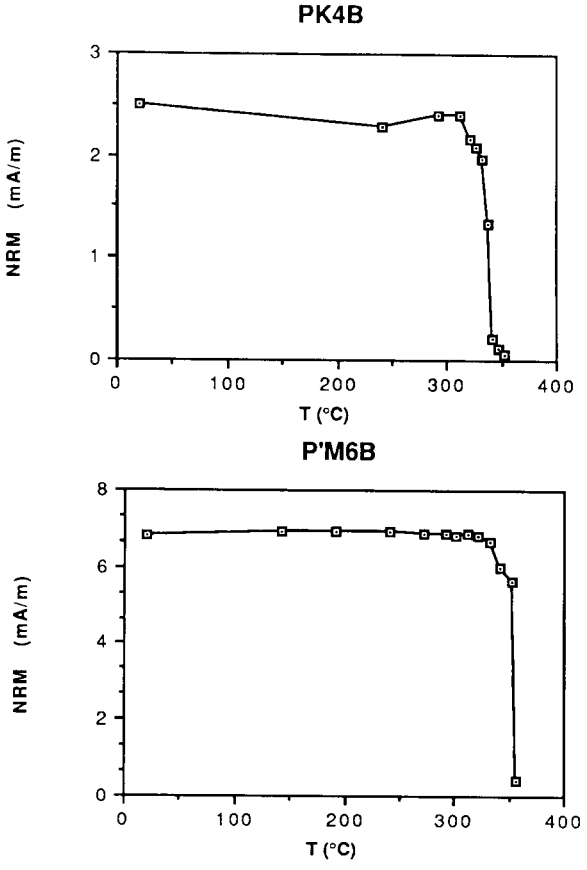

Fig. 3. Stepwise thermal demagnetization of the NRM of two samples of Jurassic limestones from the Western Alps (same location as NB10).

the fact that pyrrhotite occasionally seems to exhibit higher maximum T_b than the established Curie point at 325 °C.

In a very careful study of NRM together with artificial TRM of the Lower Jurassic schists of the internal Dauphinois zone [14] maximum T_b in the range 335–340 °C were found in a large majority of the samples but some have maximum T_b up to 350 °C (Fig. 3). Small residual remanence above 350 °C are probably due to magnetite. Those measurements were obtained in the Lamont Doherty paleomagnetic laboratory using a Schönstedt oven calibrated with a thermocouple within the samples, heated in air. Similar values of maximum T_b higher than the admitted T_c were obtained for the same rock formation with different equipment in the Gif sur Yvette, Zürich and Santa Barbara laboratories (same procedure as in Lamont except in Santa Barbara where continuous high temperature measurements were performed under argon), therefore ensuring that no instrumental error can explain these puzzling results. In particular repeated acquisition and demagnetization of TRM show completely reversible behavior. Unfortunately it is not possible to obtain thermomagnetic curves for these samples as their induced magnetization is strongly dominated by paramagnetic minerals due to very low amount of pyrrhotite.

4. The low-temperature transition of pyrrhotite

At room temperature the spontaneous magnetization of pyrrhotite is practically confined to the basal plane, perpendicular to the pseudo-hexagonal c-axis. However, M_s along the c-axis increases progressively with decreasing temperature with a discontinuity near 30 K (−243 °C) [25,26]. This discontinuity is also monitored through specific heat and electrical conductivity measurements. It was related by Besnus and Meyer [26] to a second-order transition in Fe_7S_8 but has since received no more attention by solid physicists and rock magnetists until it was rediscovered in rock samples [27]. The magnetic expression of this transition was reconfirmed more precisely in the monocrystal used by Pauthenet [25] (Table 1, [28]). The transition has a drastic effect on coercivity: measured along the c-axis of the monocrystal it increases from 10 mT above the transition to 100 mT below the transition (Fig. 4). A change of the easy axis of magnetization, possibly due to a change in electronic structure, may be suspected by analogy with the Verwey transition.

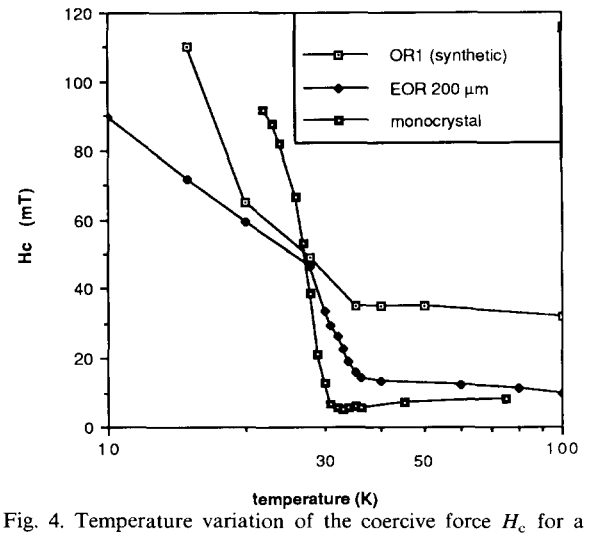

Fig. 4. Temperature variation of the coercive force H_c for a pyrrhotite monocrystal along c axis and for two dispersed powders (Table 1). H_c is almost constant between 100 K and room temperature.

Both features predict a large effect of the transition on the remanence as is shown by the thermal behavior of the saturation IRM induced at room temperature in 4 T along the easy plane of the monocrystal (Fig. 5). All subsequent experiments on remanence were obtained with a SHE cryogenic magnetometer allowing measurement of 1 cm^3 samples at variable field (0–4 T) and temperature (2–400 K) with a sensitivity of 10^{-4} A m^{-1}. After a large gradual decrease on cooling in zero field saturation IRM changes sign at 30 K. This inversion, similar to the one observed in a magnetite monocrystal near the Verwey transition [29] is partly reversible upon heating. The transition temperature (T_π) is slightly higher in a synthetic powder and three well-characterized sized dispersed powders of pyrrhotite from natural ores (Table 1, curves in [30]). These disoriented powders exhibit no inversion but a still obvious jump in coercive force (Fig. 4) and room temperature saturation IRM.

The study of room temperature saturation IRM of the sized fractions TTE and EOR, reported in [30], have shown that the transition temperature does not depend on grain size but that the reversi-

bility of the transition does. This can be appreciated either by the ratio of the heating over cooling step at T_π, h/c estimated as in Fig. 5, or by the ratio R of IRM after and before cycling. Both parameters show a coherent trend with grain size (Fig. 6), and approximatively tend to 1 (complete reversibility) for the finer grain size and to 0.5 for large multi-domain, matching the observed value of h/c of the monocrystal.

A surprising property of pyrrhotite below the transition is that the single- to multi-domain size threshold increases drastically, in agreement with the increase in coercivity. This is evidenced by the temperature dependence of M_{rs}/M_s which increases abruptly below the transition up to 0.6–0.65 at liquid helium temperature for various grain size (TTE, EOR and the synthetic powder OR1).

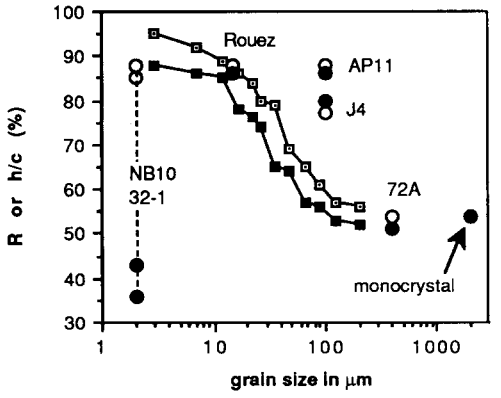

Fig. 6. Grain-size dependence of recovered fraction (R, full symbol) of the saturation IRM after liquid helium temperature cycling and of the ratio h/c defined in Fig. 5 (open symbol) for the two sized fraction TTE and EOR ([30]; squares joined by solid line) together with some other samples from this study (circles; grain size range estimated from thin section or deduced from inferred domain state; see Table 1).

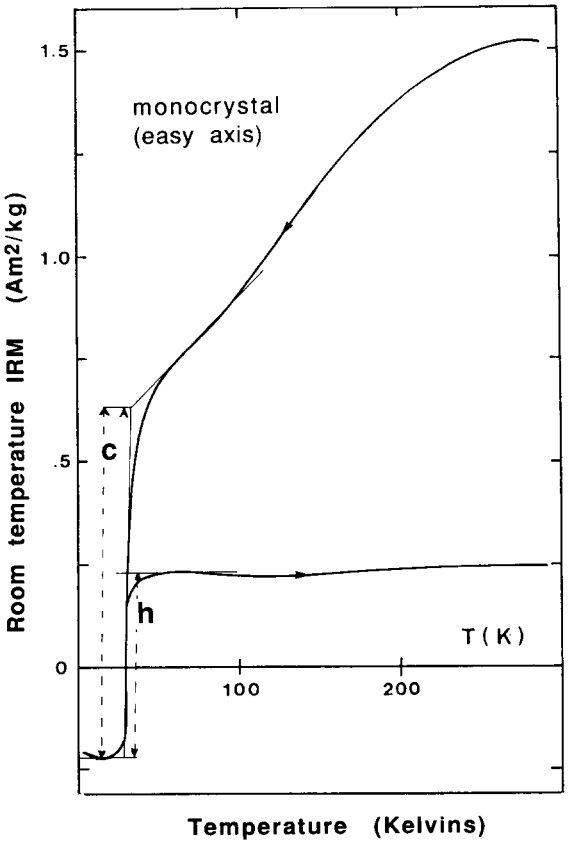

Fig. 5. Thermal variation in zero field on cooling and heating of saturation IRM acquired at room temperature within the easy plane of a pyrrhotite monocrystal.

It seems that even the 150–250 μm fraction is practically single-domain at 4.2 K [30].

5. Identification of pyrrhotite in rocks using the low-temperature transition

To show that this sharp transition on remanence can be easily recognized in rocks, a large variety of samples was studied using the same procedure. Three samples (J4, AP11 and 72A; Table 1) contain a few percent of large multi-domain pyrrhotite grains with low remanent coercive force ($H_{cr} < 30$ mT, see Fig. 2) clearly identified by thermomagnetic curves (Fig. 1) and microscopic observations. J4 and AP11 are black schists samples where pyrrhotite is due to the metamorphic breakdown of pyrite in the amphibolite facies [9,31] while 72A is a granite sample. During cycling of room temperature saturation IRM the following features are observed (Fig. 7 and Fig. 8a): a broad maximum near 200–250 K, a very well defined discontinuity with an inflection point at T_π, and a partial recovery upon heating up to room temperature. Almost identical curves were observed in four different dispersed powders (e.g. [30], Table 1). The observed maximum in the 200 K range is in fact another characteristic feature of pyrrhotite, corresponding to a maximum in M_s [6,25,30]. The rock samples exhibit $h/c = R$, as the dispersed powders (Fig. 6). While the granite

sample has values typical of its observed large grains (0.54), J4 and AP11 yield values corresponding to grain size of 20–40 μm, a figure quite small compared to estimation from coercive force or microscopic observation. The fact that the grains of those schists are strongly oriented, the measurements being done along the maximum susceptibility axis, may prevent direct comparison with unoriented powders.

Two other samples (NB10 and 32-1, Table 1) contain very small amounts of magnetic material according to the saturation IRM intensity. Both are slightly metamorphosed black shaly limestones where pyrrhotite is supposed to be derived from primary magnetite [9,19]. The value of H_{cr} is approximately 200 mT for both samples. Their NRM is hardly demagnetized in AF up to 100 mT (Fig. 2) and shows a very narrow blocking temperature spectrum upon stepwise thermal demagnetization (NB10 comes from the same formation as samples of Fig. 3). This is typical for a single-domain to pseudo-single-domain state, i.e. a grain size less than 10 μm. During liquid helium temperature cycling they show very similar room temperature saturation IRM behavior (Fig. 7), quite different from that of the previous samples. The maximum near 250 K is also present in the NB10 and 32-1 curves but the gradual remanence decrease above the transition temperature is larger and the remanence discontinuity at the transition is smaller than in the J4 and AP11 curves. h/c values are less than 0.5 and very different from R values; this is in high contrast with the behavior of the other samples and shows that the grain size chart of Fig. 6 cannot be completely generalized. However the presence of the transition at 34 K strongly confirms the identification of pyrrhotite in these rocks which have maximum unblocking temperatures up to 350 °C, higher than the established Curie point at 325 °C.

Other samples from similar formations in the Alps and Himalaya have yielded the low temperature transition of pyrrhotite. An interesting case is exemplified by sample 48 in Fig. 8b where magnetite also is identified by its Verwey transition. Such an association seems quite common and is easily detected using the low temperature technique. Concerning the detection threshold we were able to identify the transition in limestones with room temperature saturation IRM equal to 5×10^{-2} A m^{-1}, corresponding to a pyrrhotite amount of the order of 10^{-5}. Identification of previously unnoticed small amounts of pyrrhotite may therefore be expected in many instances.

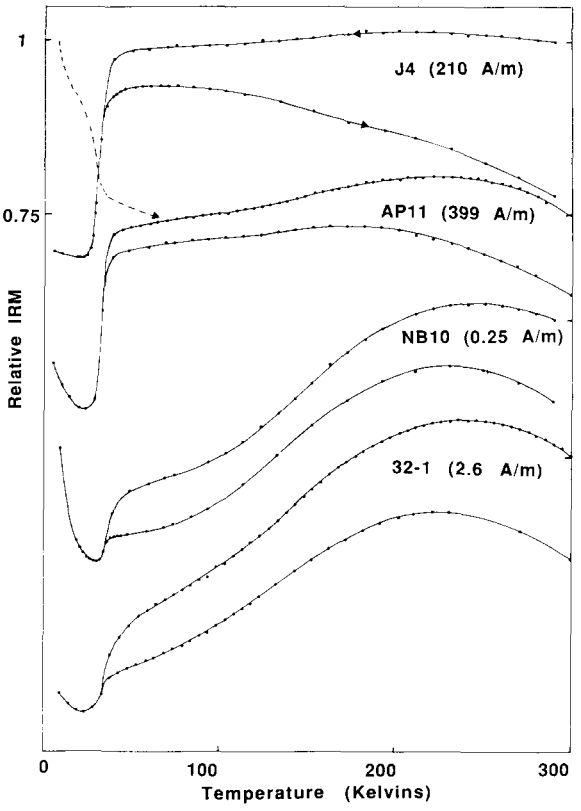

Fig. 7. Normalized thermal variation of room temperature saturation IRM (intensity indicated in brackets) upon cooling and heating for different pyrrhotite-bearing rock samples (see text). The dashed line for J4 indicates the heating curve of liquid helium temperature saturation IRM. The hyperbolic increase below 25 K probably corresponds to a small paramagnetic term caused by incomplete cancelling of the field in the magnetometer (the uncertainty is in the order of 10^{-5} T).

The transition was also detected on heating of a liquid helium temperature saturation IRM in sample J4, though its expression is less defined (Fig. 7, dashed curve). A decrease in low field susceptibility, as well as in coercivity, could also be used to trace the transition as shown by measurements on the monocrystal. But at 30 K the paramagnetic susceptibility of rocks [24] is usually already large (up to 10^{-2} SI) compared to a contribution of the order of 10^{-3} SI for 1% of pyrrhotite. Overall, liquid helium temperature cycling of IRM acquired at room temperature appears to be the most suit-

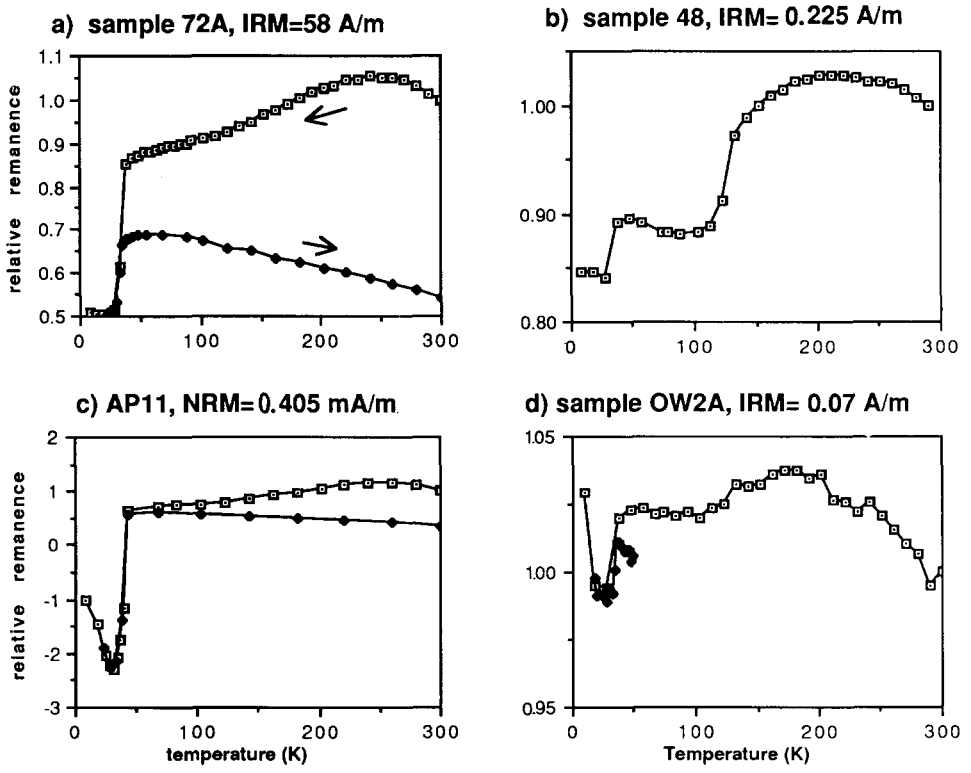

Fig. 8. Other examples of low temperature behavior of room temperature saturation IRM, except (c) where NRM is studied. (a) Hercynian granite 72A; (b) magnetite+pyrrhotite bearing limestone from Himalaya; (c) NRM of AP11 (room temperature saturation IRM is shown in Fig. 7); and (d) Appalachian limestone OW2 [33].

able procedure to demonstrate this transition in rocks. The last example—sample AP11 in Fig. 8c—shows that the transition can be also evidenced on NRM. The effect is larger than for saturation IRM and results in a reversible change of sign, as in the monocrystal. AF and stepwise thermal demagnetization of this NRM show no evidence of a reverse component that may be enhanced by the transition. Therefore it seems to be linked to an intrinsic property of the transition or to some kind of interaction with the hexagonal phase, quite abundant in this sample (Fig. 1).

6. Discussion

Precise and completely unequivocal assignment of the rock magnetic properties of pyrrhotite may be prevented by the fact that this mineral exhibits various superstructures with slightly different stoichiometry, which may be interlayered at the submicronic scale. This fact and the generalized twinning around the c-axis also suggests that the usual multi-domain theory may not be applied to pyrrhotite as the boundaries between twins or superstructures could act as fixed domain walls [11]. Characteristics of samples NB10 or 32-1 such as their quite particular low-temperature behavior, their abnormally high coercive force and maximum unblocking temperature, could point toward a different kind of pyrrhotite. Fortunately they still exhibit the low-temperature transition, thus showing that it is quite robust versus compositional changes. Whether the small but significant variation of T_π between 30 and 34 K (Table 1) is related to slight compositional change in Fe–S stoichiometry or to substitution of metallic ions, either magnetic (Ni, Mn, Co) or non-magnetic (Cu, Zn) remains to be investigated.

It is not known if the high T_b samples also yield a high T_c; however continuous measurements

at high temperature show that a remanence is still measurable above 325 °C. Explanations for this increase of the order disorder temperature must take into account that it may not be properly a magnetic transition (spin order) but a structural one due to the ordering of the iron vacancies [1]. If something prevents the diffusion of vacancies the activation energy to break the order may be enhanced. As a suggestion can be mentioned the presence of other ions or molecules in the vacancies. Oxygen may be a candidate as it has been shown that it diffuses easily in the pyrrhotite lattice, producing change in the magnetic properties, including the appearance of magnetite lamellae within the crystals [32].

Such unusually high unblocking temperature suggests to reinterpret studies where titanomagnetite was inferred from $T_b \leq 350$ °C. For example, in a study of Appalachian Silurian limestones [33], pyrrhotite was rejected as the magnetic carrier because the measured T_b were too high. A sample of these limestones was found to yield the characteristic transition of pyrrhotite (Fig. 8d). The curve, although noisy due to a very low saturation IRM intensity, seems to show also a Verwey transition, in agreement with thermal demagnetization of saturation IRM [33].

What actually happens to the spontaneous magnetization of a pyrrhotite monocrystal at the transition is still unresolved. However a change of easy axis direction within the plane perpendicular to c is in qualitative agreement with the data. There have been contradictory results on the within plane type of magnetic symmetry of pyrrhotite, which may be 2, 6 or 2 + 4 fold. This is likely to interfere in particular with the reversibility of the room temperature saturation IRM. Complete reversibility may be favored by uniaxial anisotropy, enhanced by stress or shape effect, thus suggesting that the observed grain size dependence may be related to the type of anisotropy rather than to the number of domains. On the other hand there is some evidence for the irreversibility to be linked to a rearrangement of the more mobile domain walls: after cycling the residual saturation IRM appears more difficult to AF demagnetize (Fig. 2 and [28]). However the difference is quite small and the use of liquid helium temperature cycling as a demagnetization method in pyrrhotite bearing rocks is hard to evaluate [34].

7. Conclusions

A new way to identify pyrrhotite in rocks is described, using low-temperature behavior characterized by a magnetic transition at 30–34 K and a maximum of spontaneous magnetization around 200 K. Cycling of room temperature saturation IRM down to liquid helium temperature provides a very powerful tool to detect pyrrhotite even in weakly magnetic rocks. It may also provide grain size or domain state informations. Low-temperature techniques, previously usable only for magnetite and hematite [35], are now extended to pyrrhotite (this study) and goethite [36], thus providing a complete palette that may motivate a revival of these techniques in rock magnetism. The most suitable instruments available now are the cryogenic susceptometers widely used in Solid State Physics in particular for the characterization of superconducting materials. However existing rock magnetic instruments may be adapted to allow for a liquid helium socket. Alternatively the most generally practical method is to observe the remanence behavior during rewarming of samples cooled to liquid helium temperature using cryogenic magnetometers suited for routine paleomagnetic measurements. One must be aware of potential hazards linked with the use of liquid helium and always precool devices in nitrogen.

Unblocking temperatures as high as 350 °C are demonstrated in pyrrhotite-bearing samples. This unexplained discrepancy with the currently accepted Curie point (325 °C) nevertheless suggests to reinterpret identification of titanomagnetite in some paleomagnetic studies. In the future the role of pyrrhotite in the NRM of rocks should be checked more carefully as this mineral appears to be much more important in paleomagnetic studies than previously recognized. It is also desirable to improve our ability to identify other magnetic sulfides, especially greigite and related authigenic sulfides which recently appear as important magnetic minerals in sediments and soils with eventual biogenic origin [37].

Acknowledgements

Erwin Appel, Ahmed Arafa and Dennis Kent are deeply thanked for providing their rock samples, together with Colette Maurel who prepared

the synthetic powder. The first author is greatly indebted to Mike Fuller, Dennis Kent, Carlo Laj and Bill Lowrie, whose laboratory equipments have been used for the thermal demagnetization, together with Prof. R. Hatcher for his help during the field trip in Tennessee. Various reviewers including Bill Lowrie and M. Prévot are acknowledged for their help in improving the manuscript. CNRS-INSU contribution 133 (DBT instabilités 1989).

References

1 J.C. Ward, The structure and properties of some iron sulfides, Rev. Pure Appl. Chem. 20, 175–206, 1970.
2 E.J. Schwarz, Magnetic properties of pyrrhotite and their use in applied geology and geophysics, Geol. Surv. Can., Pap. 74–59, 1975.
3 W. Lowrie and F. Heller, Magnetic properties of marine limestones, Rev. Geophys. Space Phys. 20, 171–192, 1982.
4 D.A. Clark, Hysteresis properties of sized dispersed monoclinic pyrrhotite grains, Geophys. Res. Lett. 11, 173–176, 1984.
5 M.J. Dekkers, Magnetic properties of natural pyrrhotite part 1: behavior of initial susceptibility and saturation-magnetization related parameters in a grain-size dependent framework, Phys. Earth Planet. Inter. 52, 376–393, 1988.
6 M.J. Dekkers, Magnetic properties of natural pyrrhotite part 2: high and low temperature behavior of J_{rs} and TRM as function of grain size, Phys. Earth Planet. Inter. 57, 266–283, 1989.
7 W. O'Reilly, Rock and mineral magnetism, Blackie, Glasgow, 220 pp, 1984.
8 A.J. Hall, Pyrite–pyrrhotite redox reactions in nature, Mineral. Mag. 50, 223–229, 1986.
9 P. Rochette, Metamorphic control of the magnetic mineralogy of black shales in the Swiss Alps: toward the use of magnetic isograds, Earth Planet. Sci. Lett. 84, 446–456, 1987.
10 O. Jover, P. Rochette, J.P. Lorand, M. Maeder and J.L. Bouchez, Magnetic mineralogy of some granites from the French Massif Central: origin of their low field susceptibility, Phys. Earth Planet. Inter. 55, 79–92, 1989.
11 H.C. Soffel, Domain structure of natural fine-grained pyrrhotite in a rock matrix (diabase), Phys. Earth Planet. Inter. 26, 98–106, 1981.
12 J.P. Lorand, Caractères minéralogiques et chimiques généraux des microphases du système Cu–Fe–Ni–S dans les roches du manteau supérieur: exemple d'hétérogénéité en domaine continental, Bull. Soc. Géol. Fr. 8, III, 643–655, 1987.
13 P.N. Shive and D.M. Fountain, Magnetic mineralogy in an Archean crustal cross section, J. Geophys. Res. 93, 12177–12186, 1988.
14 J.H. Linssen, Preliminary results of a study of four successive sedimentary reversal records from the Mediterranean, Phys. Earth Planet. Inter. 52, 207–231, 1988.
15 J.W. Morse, F.J. Millero, J.C. Cornwell and D. Rickard, The chemistry of hydrogen sulfide and iron sulfide systems in natural waters, Earth Sci. Rev. 24, 1–42, 1987.
16 R. Kligfield and J.E.T. Channel, Widespread remagnetization of Helvetic limestones, J. Geophys. Res. 86, 1888–1900, 1981.
17 A.J. Hall, Gypsum as a precursor to pyrrhotite in metamorphic rocks, Mineral. Deposita 17, 401–409, 1982.
18 M.G. Moreau, V. Courtillot and J. Besse, On the possibility of widespread remagnetization of pre-Oligocene rocks from Northeast Japan and the Miocene rotational opening of the Japan Sea, Earth Planet. Sci. Lett. 84, 321–338, 1987.
19 G. Lamarche and P. Rochette, Données paléomagnétiques sur le basculement tardif de la zone Dauphinoise interne, C.R. Acad. Sci. Paris 306, 711–716, 1988.
20 E. Salmon, J.B. Edel, A. Piqué and M. Westphal, Possible origin of Permian remagnetizations in Devonian and Carboniferous limestones from the Morrocan Anti-Atlas and Meseta, Phys. Earth Planet. Inter. 52, 339–351, 1988.
21 J. King, S.K. Banerjee, J. Marvin and Ö. Özdemir, A comparison of different magnetic methods for determining relative grain-size of magnetite in natural materials: some results from lake sediments, Earth Planet. Sci. Lett. 59, 404–419, 1982.
22 M. Fuller, S. Cisowsky, M. Hart, R. Haston, E. Schmidke and R. Jarrard, NRM:IRM(S) demagnetization plots: an aid to the interpretation of natural remanent magnetization, Geophys. Res. Lett. 15, 518–521, 1988.
23 P. Rochette and G. Fillion, Identification of multicomponent anisotropy in rocks using various field and temperature values in a cryogenic magnetometer, Phys. Earth Planet. Inter. 51, 379–386, 1988.
24 P. Rochette, Magnetic susceptibility of the rock matrix related to magnetic fabric studies, J. Struct. Geol. 9, 1015–1020, 1987.
25 R. Pauthenet, Étude magnétique d'un monocristal de pyrrhotine aux basses températures, C.R. Acad. Sci. Paris 234, 2261–2263, 1952.
26 M.J. Besnus and A.J. Meyer, Nouvelles données expérimentales sur le magnétisme de la pyrrhotine naturelle, Proc. Conf. Magn., Nottingham, 507–511, 1964.
27 P. Rochette, La susceptibilité anisotrope des roches faiblement magnétiques: origines et applications, Thèse d'Etat University of Grenoble, 195 pp., 1988.
28 G. Fillion and P. Rochette, The low temperature transition in monoclinic pyrrhotite, Int. Conf. Magn., Paris, 1988.
29 M. Ozima, M. Ozima and S. Akimoto, Low temperature characteristics of remanent magnetization of magnetite, J. Geomagn. Geoelec. 16, 165–177, 1964.
30 M.J. Dekkers, J.L. Mattéi, G. Fillion and P. Rochette, Grain-size dependence of the magnetic behavior of pyrrhotite during its low temperature transition at 34 K, Geophys. Res. Lett. 16, 855–858, 1989.
31 R.H. Carpenter, Pyrrhotite isograd in SE Tennessee and SW North Carolina, Geol. Soc. Am. Bull. 85, 451–456, 1974.
32 J. Graham, C.E. Bennett and A. Van Riessen, Oxygen in pyrrhotite: 1. Thermomagnetic behavior and annealing of pyrrhotites containing small quantities of oxygen, Am. Mineral. 72, 599–604, 1987.

33 S. Tucker and D.V. Kent, Multiple remagnetizations of lower Paleozoic limestones from the Taconics of Vermont, Geophys. Res. Lett. 15, 1251–1254, 1988.
34 R.T. Merril, Low temperature treatment of magnetite and magnetite bearing rocks, J. Geophys. Res. 75, 3343–3349, 1970.
35 T. Nagata, K. Kobayashi and M.D. Fuller, Identification of magnetite and hematite in rocks by magnetic observations at low temperature, J. Geophys. Res. 69, 2111–2120, 1964.
36 P. Rochette and G. Fillion, Field and temperature behavior of remanence in synthetic goethite: paleomagnetic implications, Geophys. Res. Lett. 16, 851–854, 1989.
37 F. Mann, N.H. Sparks, R.B. Frankel, D.A. Bazylinski and H.W. Jannasch, Biomineralization of ferrimagnetic greigite and iron pyrite in a magnetotactic bacterium, Nature 343, 258–260, 1990.